



ATTI
DELLA
SOCIETÀ TOSCANA
DI
SCIENZE NATURALI

MEMORIE • SERIE A • VOLUME CXXIII • ANNO 2016



Edizioni ETS



Con il contributo del Museo di Storia Naturale dell'Università di Pisa



e della Fondazione Cassa di Risparmio di Lucca

INDICE - CONTENTS

<p>F. ALQUINI, D. BERTONI, G. SARTI – Extreme erosion of a dune crest within a short timespan (January-September 2016): the recent case in the Migliarino - San Rossore - Massaciuccoli Regional Park (Tuscany, Italy). <i>Erosione molto accentuata della cresta di una duna frontale in un breve periodo di tempo (gennaio-settembre 2016): il recente caso nel Parco Regionale di Migliarino - San Rossore - Massaciuccoli (Toscana, Italia).</i></p>	pag. 5	<p>M. BELGIORNO, P. MARIANELLI, G. PASQUINI, A. SBRANA – A contribution to the study of a Pisa alluvial plain sector for low temperature geothermal assessment. <i>Un contributo allo studio di un settore della piana alluvionale di Pisa ai fini di una valutazione geotermica a bassa temperatura.</i></p>	» 17	<p>P. BILLI – Variation of the hydrological characteristics of rivers in Italy throughout the last 80 years. <i>Variazione delle caratteristiche idrologiche dei fiumi in Italia negli ultimi 80 anni.</i></p>	» 25	<p>A. COLLARETA – Fossil turtle and whale barnacles (Crustacea: Cirripedia: Coronuloidea) kept at the Natural History Museum of Pisa University: an annotated catalogue. <i>Cirripedi fossili simbionti dei vertebrati marini (Crustacea: Cirripedia: Coronuloidea) nelle collezioni del Museo di Storia Naturale dell'Università di Pisa: un catalogo annotato.</i></p>	» 41	<p>S. FARINA – Catalogue of the late Pleistocene-Holocene fossil mammalian collection from “Canale delle Acque Alte (Canale Mussolini)” (Natural History Museum, University of Pisa). <i>Catalogo della collezione a mammiferi fossili del Pleistocene Superiore - Olocene di “Canale delle Acque Alte (Canale Mussolini)” (Museo di Storia Naturale dell'Università di Pisa).</i></p>	» 47	<p>M. LEZZERINI, M. TAMPONI, G. D'AMATO AVANZI, S. IACCARINO, N. PERCHIAZZI – XRF analysis of major and minor elements in silicate rocks using fused glass discs at high dilution ratio. <i>Determinazione XRF degli elementi maggiori e minori in rocce silicatiche utilizzando dischi fusi con alti rapporti di diluizione.</i></p>	» 55	<p>S. MERLINO – OD character and polytypic features of the structure of the molecular crystal (1R,3S)-dimethyl 2-oxocyclohexane-1,3-dicarboxylate. <i>Carattere OD e aspetti politipici della struttura del cristallo molecolare (1R,3S)-dimethyl 2-oxocicloesano-1,3-dicarbossilato.</i></p>	» 61	<p>C. MONTEMAGNI, P. FULIGNATI, S. IACCARINO, P. MARIANELLI, C. MONTOMOLI, A. SBRANA – Deformation and fluid flow in the Munsiri Thrust (NW India): a preliminary fluid inclusion study. <i>Deformazione e “fluid flow” lungo il Munsiri Thrust (India NW): studio preliminare su inclusioni fluide.</i></p>	» 67	<p>N. PERCHIAZZI, P. ARMIENTI, S. IACCARINO, M. LEZZERINI – A contribution to the mineralogy of the Larderello geothermal field. X-ray crystallographic studies on borate minerals “bechilite” and “lagonite” and crystal structure determination of ginorite. <i>Contributo alla mineralogia del campo geotermico di Larderello. Studi cristallografici a raggi X dei borati “bechilite” e “lagonite” e determinazione strutturale della ginorite.</i></p>	» 79	<p>L. ROOK, Un ricordo di Augusto Azzaroli (1921-2015) <i>In memory of Augusto Azzaroli (1921-2015)</i></p>	» 89	<p>Processi Verbali - http://www.stsn.it</p>	» 101
--	--------	---	------	--	------	--	------	--	------	---	------	---	------	--	------	---	------	---	------	---	-------

CHIARA MONTEMAGNI (*) (**), PAOLO FULIGNATI (**), SALVATORE IACCARINO (**), PAOLA MARIANELLI (**),
CHIARA MONTOMOLI (**) (***), ALESSANDRO SBRANA (**)

DEFORMATION AND FLUID FLOW IN THE MUNSIARI THRUST (NW INDIA): A PRELIMINARY FLUID INCLUSION STUDY

Abstract - Deformation and fluid flow in the Munsiri Thrust (NW India): a preliminary fluid inclusion study. A fluid inclusion study was carried out on quartz veins deformed during the activity of the Munsiri Thrust in the Garhwal Himalaya (NW India, Western Himalaya). These veins are hosted in mylonitic phyllites, with a greenschist mineral assemblage made of quartz-white mica-biotite-chlorite-epidote and minor calcite and plagioclase. Within the veins two groups of isolated "early fluid" inclusions and trails of small secondary fluid inclusions have been observed.

Two types of inclusions preserved in isolated groups have been petrographically recognized: (i) a two liquids and a vapor phase (L1+L2+V) that is the most common type and (ii) a less frequent liquid and a vapor phase (L+V). Both types of fluid inclusions were investigated through optical microthermometric experiments.

For "early fluid" inclusions, assuming a trapping temperature based on quartz dynamic recrystallization mechanisms and previous P-T estimates, in the range of 500-520°C, a corresponding trapping pressure in the range of c. 0.50-0.53 GPa is estimated.

The trapping pressure range evaluated in the present contribution support that these fluid inclusions have been entrapped during the early stages of the activity of the Munsiri Thrust.

Key words - fluid inclusions, fluids and metamorphism, Munsiri Thrust, Garhwal Himalaya, Main Central Thrust

Riassunto - Deformazione e "fluid flow" lungo il Munsiri Thrust (India NW): studio preliminare su inclusioni fluide. In questo lavoro è stato condotto uno studio su inclusioni fluide preservate in vene di quarzo deformate dall'attività del Munsiri Thrust (NW India, Himalaya occidentale). Queste vene di quarzo si trovano in filladi milonitiche deformate in condizioni metamorfiche in facies scisti verdi, e sono associate alla ricristallizzazione di quarzo, mica bianca, biotite, chlorite, epidoto, calcite e plagioclasio. Lo studio petrografico ha evidenziato all'interno delle vene la presenza di gruppi isolati di inclusioni fluide oltre che inclusioni fluide allineate lungo *trails* secondari. In particolare, sono stati identificati due tipi di inclusioni preservate in gruppi isolati: (i) inclusioni trifasiche (L1+L2+V) costituite da due liquidi immiscibili e da una fase vapore e (ii) inclusioni bifasiche (L+V) costituite da una fase acquosa e da una fase vapore. Entrambi i tipi di inclusioni sono stati studiati mediante esperimenti di microtermometria ottica. Assumendo, per le inclusioni trifasiche, una temperatura di intrappolamento compresa tra 500 e 520°C, vincolata dai meccanismi di ricristallizzazione dinamica del quarzo e da dati di letteratura, è stata stimata una pressione minima di intrappolamento di circa 0.50-0.53 GPa.

La pressione di intrappolamento stimata nel presente lavoro, permette di affermare che esse sono state intrappolate durante le prime fasi di attività del Munsiri Thrust.

Parole chiave - inclusioni fluide, fluidi e metamorfismo, Munsiri Thrust, Garhwal Himalaya, Main Central Thrust

INTRODUCTION

Himalaya (Fig. 1) is characterized by the occurrence of several first order tectonic discontinuities running all over the length of the belt (Hodges, 2000). Among these regional scale discontinuities, the Main Central Thrust Zone (MCTZ), a top-to-the-S/SW regional scale shear zone dipping to the north, tectonically divides the Lesser Himalayan Sequence (LHS) in the foot-wall, from the Greater Himalayan Sequence (GHS) in the hanging-wall. The MCTZ is a wide, km-thick ductile shear zone, classically delimited by two systems of reverse faults, that in different portions of the belt are named in different ways. Arita (1983) defines as MCT-1 the structurally lower thrust and as MCT-2 the upper one of the MCTZ. Saklani *et al.* (1991) refer to the lower one as MCT2, whereas De Celles *et al.* (2000), Robinson *et al.* (2001) and Robinson (2008 and references therein) refer to it as Ramgarh Thrust and define as MCT "sensu stricto" the upper thrust, which often (*e.g.* Colchen *et al.*, 1986) is placed near the kyanite isograds. In the study area, (Garhwal region, NW India, Fig. 2) the MCT has been firstly defined by Heim & Gansser (1939), and the two bounding thrusts are named as: (i) Munsiri Thrust (MT) at the bottom (Valdiya, 1980) and (ii) Vaikrita Thrust (VT) at the top (Valdiya, 1980; Gururajan & Chaudhuri, 1999; Jain *et al.*, 2014).

More recently, several authors such as Larson & Godin (2009) re-interpreted the tectonic meaning of the Ramgarh thrust/MCT I/Munsiri structures and refer as the MCT the base of pervasively sheared rocks,

(*) Dipartimento di Scienze dell'Ambiente, del Territorio e di Scienze della Terra, Università degli Studi di Milano - Bicocca, Piazza della Scienza 4, 20126 Milano, Italy. Email: c.montemagni@campus.unimib.it

(**) Dipartimento di Scienze della Terra, Università di Pisa, via S. Maria 53, 56126 Pisa, Italy.

(***) Istituto di Geoscienze e Georisorse, via G. Moruzzi 1, 56124 Pisa, Italy.

grouped as GHS, during the Himalaya orogenesis, following the arguments of Searle *et al.* (2008). Indeed, in a review dealing with the MCT definition, Searle *et al.* (2008) pointed out how, despite the different approaches followed by several authors (e.g. Gansser, 1983; Daniel *et al.*, 2003; Bordet, 1961; Le Fort, 1975; Colchen *et al.*, 1986; Parrish & Hodges, 1996; Ahmad *et al.*, 2000; DeCelles *et al.*, 2000; Robinson *et al.*, 2001; Martin *et al.*, 2005; Richards *et al.*, 2005; Harrison *et al.*, 1997; Catlos *et al.*, 2001, 2002) can provide essential information on age, stratigraphy and metamorphism, none of these approaches can define the true location of MCT. According to Searle *et al.* (2008), the criteria to define a crustal scale shear zone as the MCT, is the identification of a strain gradient where a clear localization (evident from field and microstructural analyses) of deformation is present. Moreover, the former authors also pointed out how the MCT often corresponds strictly to the base of rocks showing an inverted metamorphism (Searle & Rex, 1989; Davidson *et al.*, 1997; Walker *et al.*, 1999; Searle *et al.*, 2008).

Martin (2016) highlighted how none of the three current definitions of the MCT (metamorphic-rheological, age of motion-structural or protolith boundary-structural) can unambiguously define the MCT. Martin (2016) suggests that the best definition of the MCT could be based on the recognition of a protolith boundary, where high-strain zone showing a reverse kinematics is present.

For these reasons, several authors (e.g. Carosi *et al.*, 2007; Iaccarino *et al.*, 2017) do not use a division based on the occurrence of two distinct thrusts, but refer collectively to these pervasive sheared rocks, with a reverse kinematics, as the MCT zone (MCTZ). One important point to stress is that the MCTZ has a composite evolution from ductile to brittle behavior and it has been active for a long span of time, mostly between ~23 and 15 Ma, in different areas of the Himalayas (Godin *et al.*, 2006 and Montomoli *et al.*, 2015 for a review).

A brittle reactivation of the MCTZ, active in more recent time after the main ductile phase has been reported for several sections along the belt (Macfarlane, 1993; Catlos *et al.*, 2002; Carosi *et al.*, 2007). How highlighted by Yin (2006), the MCT has been mapped at different structural levels, so its location could probably vary with time within the MCTZ. Moreover, recent findings (Carosi *et al.*, 2007, 2010, 2016; Corrie & Kohn, 2011; Rubatto *et al.*, 2012; Montomoli *et al.*, 2013, 2015; Iaccarino *et al.*, 2017) have reported the occurrence of others first-order contractional top-to-the S/SW shear zones within the GHS, structurally higher and older than the MCTZ. These occurrences, their ages and the metamorphic paths of the hanging-wall and footwall rocks testify how

the tectono-metamorphic history of the GHS is much more complex than previously thought. Montomoli *et al.* (2013, 2015) stressed the importance of a multidisciplinary approach, including structural, metamorphic modeling and geochronological studies, to unambiguously define a tectonic discontinuity, such as the MCT.

Metamorphism within the MCTZ was investigated and constrained in numerous transects along the belt, where P-T conditions of peak metamorphism mostly comprised between c. 0.6-1.0 GPa and 520-650°C (e.g. Hubbard, 1989; Vannay & Grasemann, 1998; Catlos *et al.*, 2001; Kohn *et al.*, 2001; Vannay *et al.*, 2004; Iaccarino *et al.*, 2017). One peculiar feature of the MCTZ, as anticipated above, is that it coincides with a zone of “inverse metamorphic grade” ranging from the biotite to the sillimanite zone moving structurally upward (e.g. Searle *et al.*, 2008; see Kohn, 2014 for an update review).

Aim of this work is to study the paleofluids circulating within the MCTZ during its activity through fluid inclusions entrapped in tectonic veins coupled with a description of the main microstructural features. In particular, we analyzed fluid inclusions entrapped in quartz veins, deformed by the Munsiri Thrust (Jain *et al.*, 2014 and references therein) in order to constrain metamorphic and fluids conditions present during the Munsiri Thrust shearing.

THE HIMALAYAN BELT: AN OVERVIEW

The Himalayan mountain belt derives from the protracted continental collision between India and Asia, occurred at 55 Ma (Yin & Harrison, 2000). The belt is build up by four main litho-tectonic units that are, from south to north, Sub-Himalaya, Lesser Himalayan Sequence (LHS), Greater Himalayan Sequence (GHS) and Tibetan Sedimentary Sequence (TSS) divided by first order discontinuities, namely the Main Boundary Thrust (MBT), the Main Central Thrust (MCT), and the South Tibetan Detachment System (STDS; Fig. 1). The Sub-Himalaya, is made up mainly by Miocene to Pleistocene sediments derived from the erosion of the belt (Dèzes, 1999). The MBT divides the Sub-Himalaya, from the overlying LHS.

The LHS is composed by quartzite, phyllite, marble, schist and orthogneiss metamorphosed from greenschist to lower amphibolitic facies (Hodges, 2000). The LHS, is separated from the overlying GHS, by the top-to-the south MCTZ.

The GHS, is a sequence of metamorphic rocks, such as gneiss, schist, migmatite and calc-silicate showing a high grade metamorphism, and oligo-miocene leucogranite (Hodges, 2000; Visonà *et al.*, 2012; Montomoli *et al.*, 2013; Carosi *et al.*, 2014).

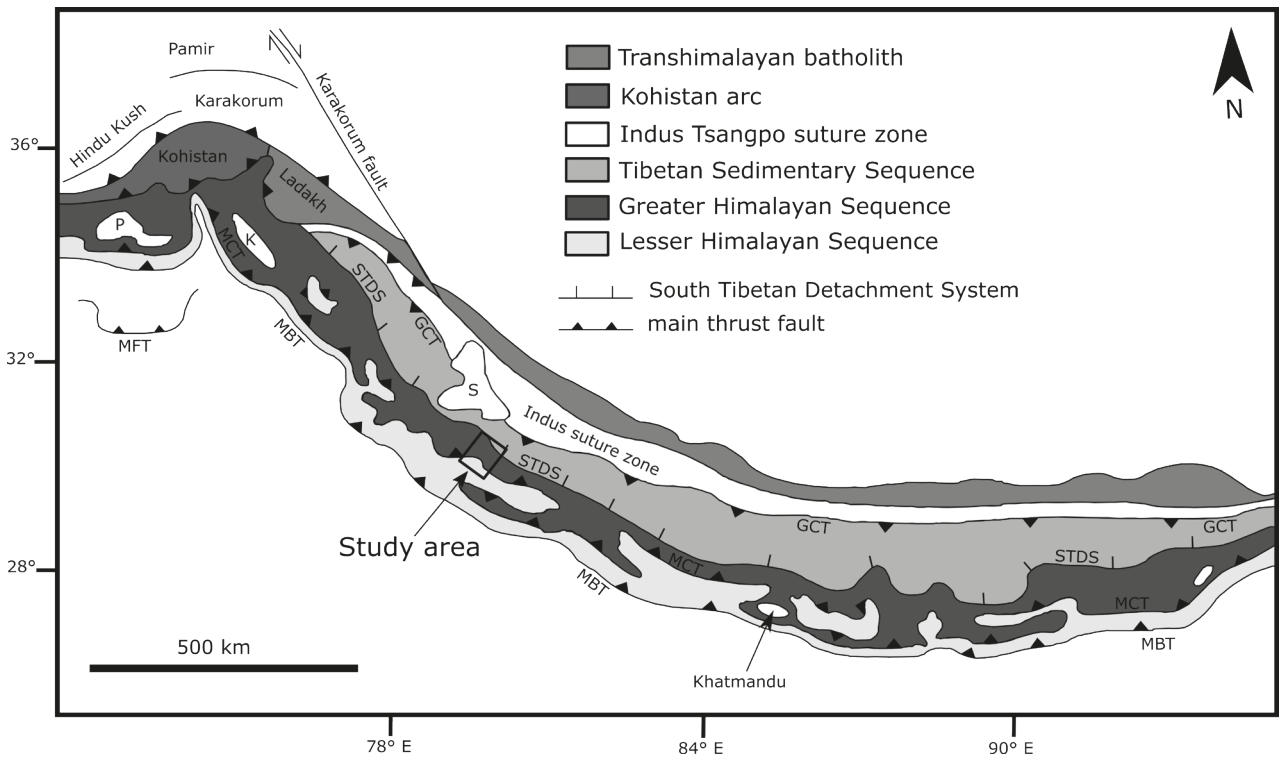


Fig. 1 - Simplified geological map of the Himalayas. MFT: Main Frontal Thrust; MBT: Main Boundary Thrust; MCT: Main Central Thrust; STDS: South Tibetan Detachment System; GCT: Great Counter Thrust; K: Kashmir Neogene basin; P: Peshawar basin; S: Sutlej basin (modified after Searle *et al.*, 2003).

Two main metamorphic events can be identified within the GHS: the first event is the main regional prograde metamorphism, associated with crustal thickening and S verging folding, the second one is related to the main exhumation period often related to isothermal decompression (Dèzes, 1999; Searle *et al.*, 2007) or decompression and heating (Groppo *et al.*, 2009; Iaccarino *et al.*, 2017). The first stage is characterized by medium to high pressure kyanite-bearing metamorphism, that started around 48-45 Ma (Carosi *et al.*, 2010, 2014, 2015; Iaccarino *et al.*, 2015) with a climax around 35-30 Ma (Vance & Harris, 1999). The second metamorphic stage is associated with medium-low pressure sillimanite to cordierite grade metamorphism in the time span of 25-18 Ma, associated with extensive partial melting and High Himalayan Leucogranite (HHL) production (Dèzes, 1999; Hodges, 2000; Searle *et al.*, 2007; Montomoli *et al.*, 2013; Iaccarino *et al.*, 2017).

The STDS, a system of a top-to-the north shear zones and faults, divides the GHS from the structurally upper TSS. This litho-tectonic unit is mainly made up by poly-deformed low-grade metamorphic rocks, such as quartzite, slates and impure limestone (Gaetani

& Garzanti, 1991; Antolin *et al.*, 2011; Dunkl *et al.*, 2011). Metamorphic conditions, up to lower amphibolite facies, are commonly observed at the base of the TSS, moving closer to the STDS, even if they have also sporadically reported (e.g. Hodges, 2000; Montomoli *et al.*, 2017) away from this tectonic contact. The TSS is tectonically bounded to the North, by the Indus Tsangpo Suture Zone (ITSZ), a discontinuous belt of mafic-ultramafic rocks and deep-water sediments, often with a high pressure-low temperature overprints, representing the suture between the Indian and Asian Plate.

STUDY AREA

The geological transect

The study area is located in the Garhwal Himalaya (Uttarakhand, NW India, Fig. 1 and 2), where a complete and well exposed structural transect across the MCTZ, located between the Helang and Joshimath villages (Fig. 2), was investigated. In the study area, structural and P-T conditions were defined by Hodges

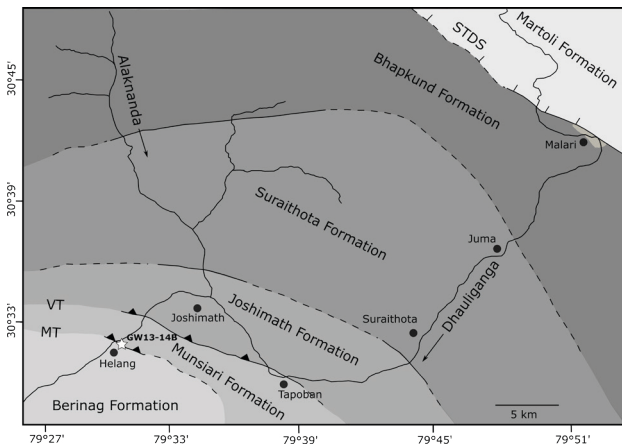


Fig. 2 - Geology in the study area, Alaknanda Dhauiliganga valleys (modified after Spencer *et al.*, 2012). White star indicates the position of the studied sample, GW13-14B.

& Silverberg (1988), Spencer *et al.* (2012), Sachan *et al.* (2010, 2013), Jain *et al.* (2014 and references therein), Sen *et al.* (2015) and Thakur *et al.* (2015).

The LHS is located in the southernmost portion of the transect, near Helang village, where Berinag Formation, crops out (Fig. 2). It mainly includes schist, quartzite and carbonate rocks showing a greenschist facies metamorphism, with the main foliation striking NW-SE and dipping 30-35° to the NE (Jain *et al.*, 2014).

At the microscale, the rocks of the Berinag Formation show a main crenulation cleavage (S2) that overprints an older foliation (S1), locally present within the microlithons and oriented at high-angle with respect to the main one. The mineral assemblage mostly consists of quartz, calcite, chlorite and white mica. Calcite porphyroblasts show type 1 and 2 twinning, according to Ferrill *et al.* (2004) classification. Quartz is affected by Subgrain Rotation (SGR) locally superimposed on Grain Boundary Migration (GBM; Passchier & Trouw, 2005). The Berinag Formation is overlain by the pervasively sheared rocks of the MCTZ. Within the MCTZ, the Munsiri Formation crops out. It is made up by pre-Cambrian orthogneiss, garnet-bearing mica schist, calc-silicate and quartzite (Jain *et al.*, 2014). The main foliation strikes from W-E to NW-SE and dips 45° from N to NE, whereas the main stretching lineation is oriented N20,45 NE. According to Jain *et al.* (2014), the main kinematic indicators at the mesoscale are well-developed S-C and S-C-C' fabrics and asymmetrically sheared boudins pointing a top-to-SW sense of shear. At the microscale, the main kinematic indicators such as S-C fabric, mica fish and σ/δ -porphyroclasts confirm a top-to-SW sense of shear. Available time constraints in the study area and nearby locality have shown that potentially, the MCTZ shearing

lasted up to c. 6 Ma, based on Th-Pb monazite ages (Catlos *et al.*, 2002). Sen *et al.* (2015) reported ^{40}Ar - ^{39}Ar ages on biotite of c. 10 Ma and on muscovite of c. 6 Ma for rocks from the MCTZ.

The Joshimath Formation, representing the lower portion of the GHS in the study area (Spencer *et al.*, 2012; Thakur *et al.*, 2015), includes pelitic schist, paragneiss and minor calc-silicate, where the main foliation strikes from WNW-ESE to NW-SE and dips 35-40° from N to NE (Jain *et al.*, 2014). At the microscale, Joshimath Formation shows a common mineral assemblage of garnet, quartz, white mica, plagioclase, biotite, staurolite and minor kyanite. The main foliation (S2) overprints an older foliation (S1), only locally preserved. Staurolite porphyroblasts are syn-kinematic and contain an internal foliation (Si) concordant with the main one. Garnet is often enveloped by the main foliation. Deformation mechanisms are represented by high temperature GBM and static recrystallisation in quartz. Kinematic indicators such as S-C-C' fabric, mica fish and σ/δ -porphyroclasts show a top-to-SW sense of shear.

Structurally upward the GHS comprises the Surraithota and the Bhapkund formations. The Surraithota Formation is mainly represented by kyanite-garnet-biotite-bearing gneiss, quartzite and schist with amphibolite intercalations (Jain *et al.*, 2014). The main foliation strikes N120°-150° with a dip of 30°-40° toward NE (Jain *et al.*, 2014). The Bhapkund Formation is made up by sillimanite-garnet-biotite migmatitic gneiss, tourmaline-rich leucogranitic pods and dikes. The Malari leucogranite (Sachan *et al.*, 2010), a small pluton with an emplacement age of c. 19 Ma (U-Pb, zircon), crops out at the northern margin of the Bhapkund Formation. According to Sachan *et al.* (2010), rocks of the Malari leucogranite consist of quartz, perthitic K-feldspar, plagioclase, muscovite and tourmaline.

Structurally upward, the Martoli formation, representing the TSS in this portion of the belt, is present. This formation is made up of a series of Neo-proterozoic clastic rocks, with a low-grade metamorphism (Sachan *et al.*, 2010; Jain *et al.*, 2014).

P-T conditions and previous fluid inclusion data of the MCTZ in the study area

Temperature conditions adjacent to the Munsiri thrust in the study area, have been previously constrained by Célérier *et al.* (2009) that report values ranging from 500 to 520°C in the LHS, based on the Raman spectroscopy of carbonaceous material (RSCM) thermometer.

Spencer *et al.* (2012) obtained P-T conditions, based on "classical" geothermobarometry, for the MCTZ between 0.5-1.1 GPa and 500-600° C from Munsiri

to the Vaikrita Thrust (Fig. 2). Data of Spencer *et al.* (2012) are in agreement with Thakur *et al.* (2015) that obtained P-T conditions of 0.63-0.75 GPa and 550-582°C within the MCTZ through pseudosection modeling and multi-equilibrium thermobarometry.

Sachan *et al.* (2001) analysed CO₂ - H₂O fluid inclusions from two transects in the Bhagirathi valley (about 100 km westward of the study area). P-T values obtained by microthermometric analyses on these inclusions are 0.44 GPa and 548°C for Munsiri and 0.48 GPa and 562°C for Vaikrita Thrust, with an increase in the CO₂ content related to the increase in the metamorphic grade. The same authors reported also temperature values of c. 530-550°C, and pressure values from c. 0.5 to 0.8 GPa obtained with “classical” geothermobarometry.

In the study area, Sachan *et al.* (2013) investigated fluid inclusions trapped in quartzitic pelite of the middle portion of GHS, in order to define the types of fluids

present during quartz recrystallization. This contribution reports three types of fluid inclusions: high-salinity brine, CO₂-H₂O and H₂O-NaCl, the latter being involved in recrystallization processes at P-T values of 0.05-0.48 GPa and 350-430°C. Moreover, Spencer *et al.* (2011) reported high salinity three-phase fluid inclusions within quartz grains from the middle portion of the GHS.

Sen *et al.* (2015) petrographically described fluid inclusions hosted in quartz boudins of middle portion of the GHS (near Surathota, Fig. 2) and in the Malari leucogranite. The fluid inclusions trapped in quartz of the GHS form secondary trails that cross-cut subgrain boundaries and were interpreted by Sen *et al.* (2015) to be late features formed below 400°C. Moreover, these fluid inclusions show decrepitation textures formed probably during an isothermal decompression (Sen *et al.*, 2015). The fluid inclusions trapped in quartz from the Malari leucogranite are annular fluid inclusions forming secondary trails cross-cutting subgrain boundaries and showing decrepitation textures that suggest implosion processes (Sen *et al.*, 2015).



Fig. 3 - Outcrop of the Munsiri Thrust. Well-developed S-C fabric and sigmoidal quartz aggregates show a top-to-SW sense of shear.

STRUCTURAL AND PETROGRAPHIC FEATURES OF THE STUDIED VEINS AND HOST ROCKS

A set of syn-tectonic veins has been studied due to their structural features (Fig. 3). They are quartz veins characterized by a sigmoidal shape acquired during the activity of the Munsiri Thrust (Fig. 3). These veins are made mostly of quartz and minor amounts of calcite. They have been selected for the abundance and for the features of the fluid inclusions, such as their size, shape and the lacking of decrepitation features.

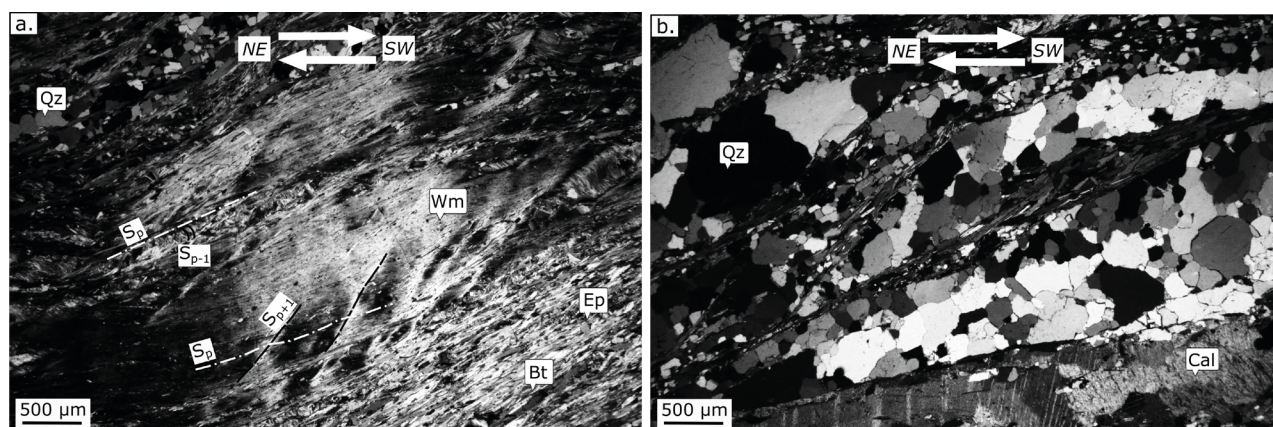


Fig. 4 - a: microscopical aspect of the mylonitic phyllitic host rocks of the quartz veins. The main foliation (S_p), the older foliation (S_{p-1}) and the late crenulation cleavage (S_{p+1}) are highlighted. b: S-C fabric showing a top to SW sense of shear. Note the GBM in quartz and type-1 & 2 twinning in calcite. Mineral abbreviations: Qz=quartz; Wm=white mica; Ep=epidote; Bt=biotite; Cal=calcite.

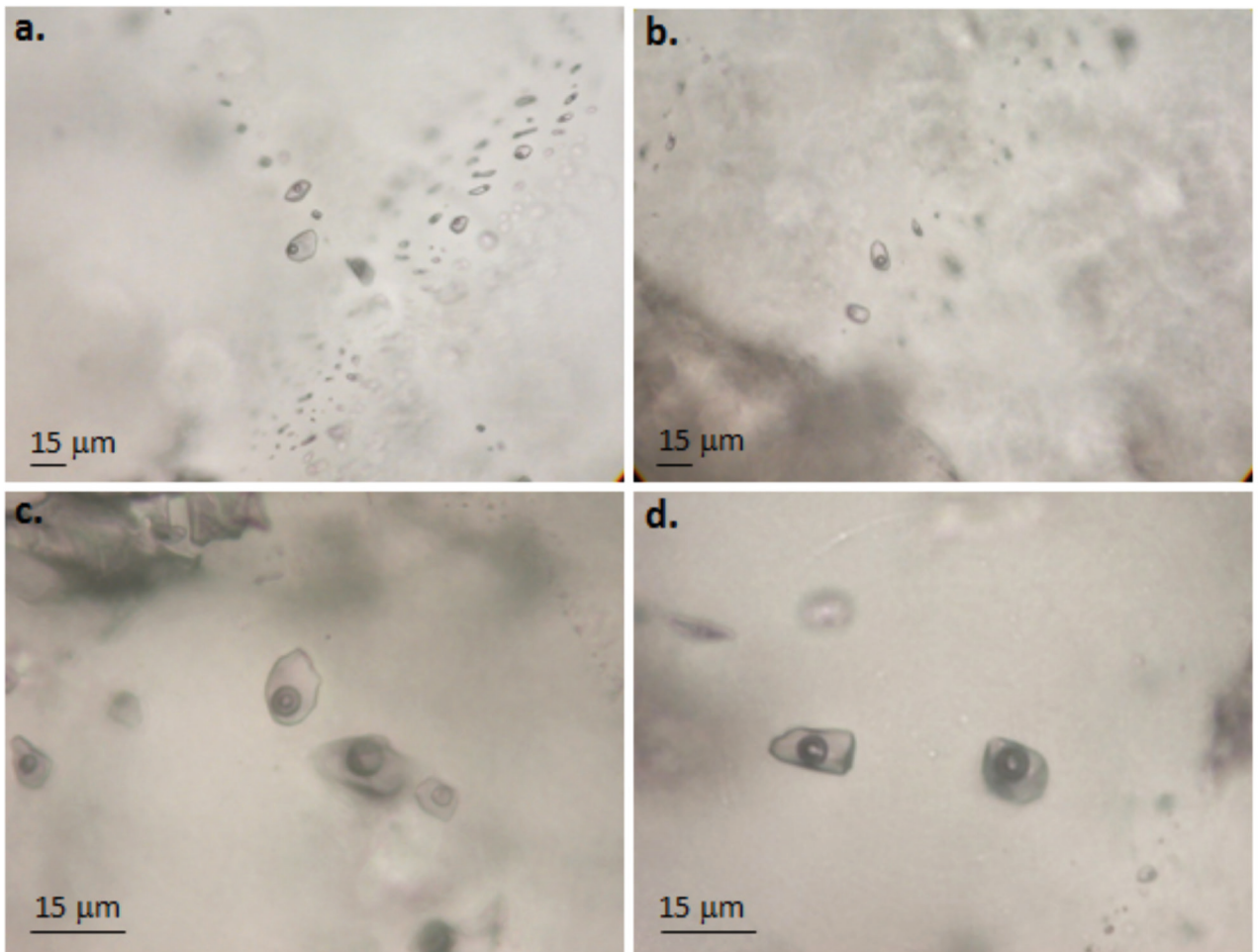


Fig. 5 - a: oblate and tubular shaped fluid inclusions, forming secondary trails. b: isolated group of “early fluid” inclusions. c: analysed oblate tri-phase and two-phase early fluid inclusions. d: L1+L2+V fluid inclusions.

At the microscale, the veins show a mosaic texture and quartz displays evidence of GBM: it shows undulose extinction and amoeboid grain boundaries. According to Stipp *et al.* (2002), GBM implies a minimum recrystallization temperature of 500°C.

The host rocks are phyllites made up by quartz, white mica, biotite, chlorite, epidote and minor calcite and plagioclase. At the outcrop scale well-developed S-C fabric and sigmoidal quartz aggregates (Fig. 3) are present, pointing a top-to-the S/SW sense of shear. At the microscale, selected phyllitic sample shows (Fig. 4a) a main spaced foliation (S_p) made by the alternation of lepidoblastic layers, and quartz and calcite granoblastic ones. S_p is irregular and made up by discontinuous layers variable in thickness, forming an anastomosing mylonitic foliation. Locally, in the microlithons, an older foliation is present (S_{p-1}), marked by micas oriented at high-angle with respect to the main foliation (Fig. 4a). A

late mild gradational crenulation cleavage (S_{p+1}) is locally present, not associated with dynamic recrystallization of micas (Fig. 4a). One striking feature is the presence of larger post-kinematic white mica clearly overprinting S_p and S_{p-1} , but with no resolvable relationship with S_{p+1} . Deformation mechanisms are represented by GBM in quartz (Fig. 4b) and type 1 and 2 twinning in calcite crystals (Ferrill *et al.*, 2004). Kinematic indicators such as type 2 mica fish (Passchier & Trouw, 2005) S-C fabric (Fig. 4b), drag folds and sigmoidal quartz aggregates show a top-to-SW sense of shear.

FLUID INCLUSION DATA

A fluid inclusion study has been carried out on one selected sample, GW13-14B (Fig. 2), coming from the sigmoidal quartz veins deformed by the MT (Fig. 3).

Tab. 1 - Summary of microthermometric data. $T_{m\text{ ice}}$: ice melting temperature; $T_{d\text{ cl.}}$: clathrate dissociation temperature; $T_{h\text{ CO}_2}$: CO_2 homogenization temperature (in liquid phase); $T_{h\text{}}$: total homogenization temperature (in liquid phase); L: homogenization to the liquid phase; no.: number of measurements.

FLUID INCLUSION TYPE		$T_{m\text{ ice}}$ (°C)	$T_{d\text{ cl.}}$ (°C)	$T_{h\text{ CO}_2}$ (°C)	$T_{h\text{}}$ (°C)
L1+L2+V	MIN/MAX	-65.4/-30.0	5.5/8.8	22.5/29.9 (L)	190.0/308.9 (L)
	NO.	43	50	72	64
L+V	MIN/MAX	-53.1/-23.3	3.0/11.1	/	194.6/320.1 (L)
	NO.	12	14		15

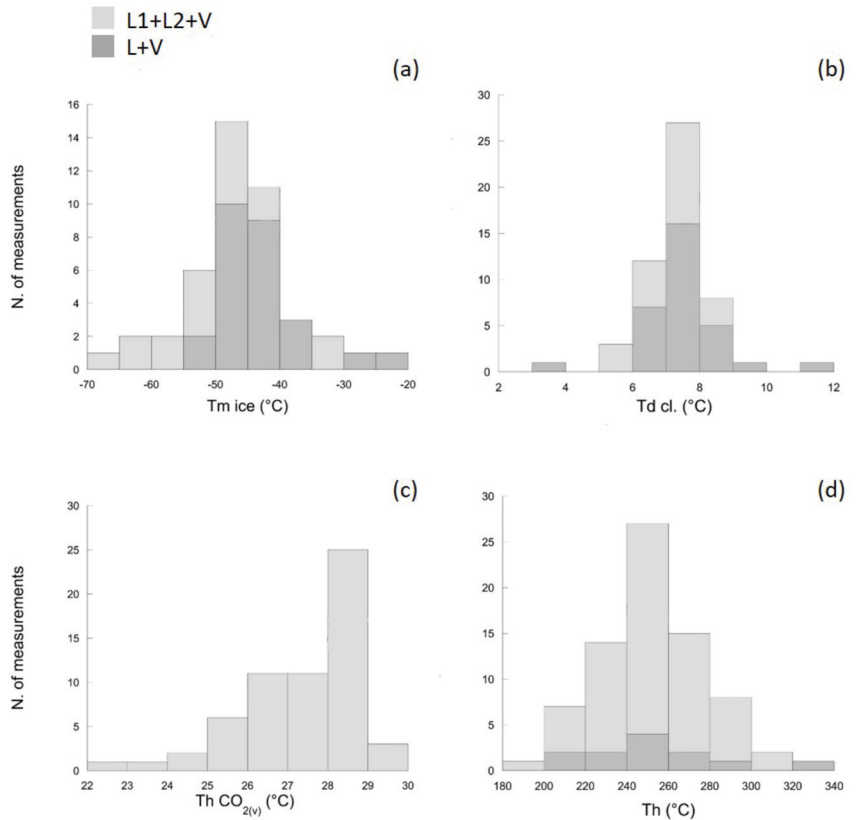


Fig. 6 - Histograms reporting microthermometric data obtained on L1+L2+V and L+V on quartz syntectonic vein of the Munsiri Thrust. (a): ice melting temperature ($T_{m\text{ ice}}$); (b): clathrate dissociation temperature ($T_{d\text{ cl.}}$); (c): CO_2 vapour bubble homogenization temperature ($T_{h\text{ CO}_2(v)}$); (d): total homogenization temperature ($T_{h\text{}}$).

Doubly polished thin sections (100-300 μm thick) were prepared for petrography and microthermometric determinations. Microthermometric measurements were carried out using a Linkam THMS 600 heating-freezing stage at the Earth Science Department of Pisa University. The accuracy of measurements was $\pm 2^\circ\text{C}$ at 398°C controlled by the melting point of $\text{K}_2\text{Cr}_2\text{O}_7$, $\pm 0.1^\circ\text{C}$ at 0°C and $\pm 0.2^\circ\text{C}$ at -56.6°C controlled by using certified pure water and CO_2 -bearing synthetic fluid inclusions (Synthetic Fluid Inclusion Reference Set, Bubbles Inc., USA). Salinities of fluid inclusions are reported in weight percent NaCl equivalent (wt.% NaCl_{eq}), based on clathrate melting temperatures and using the equation of Darling (1991) for the $\text{H}_2\text{O}-\text{CO}_2\text{-NaCl}$ system. In the sample, there are both “early fluid” inclusions

(*sensu* Touret, 2001) and secondary fluid inclusions (Fig. 5a, b). The formers are relative to the earlier phases of host mineral deformation, they are mostly oblate in shape (15-20 μm ; Fig. 5b, c, d), isolated or preserved in small groups (Fig. 5b) far from boundary grains; the latter trapped during the later stages of deformation and are preserved along secondary trails (Fig. 5a). These inclusions are oblate and smaller than the others (2-3 μm). Only the “early fluid” inclusions have been analyzed, due to the small size of the others. Two types of “early fluid” inclusions have been recognized:

(i) *Immiscible liquid tri-phase (L1+L2+V) inclusions*, characterized by two immiscible liquids, one aqueous and the other one CO_2 -rich (Fig. 5c, d). These inclusions are the most abundant type in the sample.

(i) *Liquid-rich, two-phase (L+V) inclusions*, are water-rich inclusions made of by an aqueous liquid and a vapor phase (Fig. 5c).

Volumetric proportions between aqueous and vapor phases in the inclusions were estimated through the free software ImageJ (Schneider *et al.*, 2012). For both tri-phase and two-phase inclusions liquid/vapor ratio is constant and varies mostly between 80-95% and 80-88% for tri-phase and two-phase inclusions, respectively. The tri-phase inclusions mainly occur as “early fluid” inclusions, whereas the two-phase inclusions are prevalent in secondary trails.

The microthermometric results are reported in Tab. 1 and Fig. 6.

Upon freezing, tri-phase inclusions are characterized by clathrate formation, whose dissociation temperatures ($T_{d.cl.}$) range between 5.5° and 8.8°C, with a modal value around 7.5°C. The salinity ranges between 2.4 and 8.3 wt.% NaCl_{eq}. Final ice melting temperatures ($T_{m.ice}$) range from -65.4° and -30.0°C; CO₂ vapor bubble homogenization temperatures (T_h CO₂) are comprised between 23° and 30°C, with a modal value at 28.5°C. Tri-phase inclusions homogenize (T_h) to the liquid phase mostly between 200° and 300°C, with a modal value around 250°C. Decrepitation phenomena occur for some inclusions, above 270°C.

In two-phase inclusions, the $T_{m.ice}$ ranges between -53.1° and -23.3°C. The clathrate dissociation occurs between 3.0° and 11.1°C with a modal value at 7.5° C, corresponding to a salinity range between 2.4 and 11.9 wt.% NaCl_{eq}. On heating, some inclusions show bubble enlargement before homogenization to liquid phase, which in the other inclusions occurs between 195° and 320°C.

DISCUSSION AND CONCLUSIONS

Fluid inclusion data are used for the evaluation of P-T-X conditions of fluids circulated during the activity of the Munsiri Thrust.

CO₂ molar volume (V_m) and CO₂ molar fraction (X_m) were estimated from tri-phase fluid inclusion data using the Bakker & Diamond (2000) model for H₂O - CO₂ system. This allows to determine molar volume and molar fraction of CO₂ in the fluid inclusions, knowing the temperature of partial homogenization of the CO₂ and the total homogenization temperature. Thus, only L1+L2+V inclusions have been considered to constrain the P-T values. Assuming the homogenization temperature of CO_{2(v)} to CO_{2(l)} to be 28°C, and a total homogenization temperature of 250°C, CO₂ molar volume results 23.5 cm³/mol and its molar fraction 0.12. The fluid inclusions trapping conditions

have been obtained with the software ISOC (Bakker, 2003), using the equation of state reported in Jacob & Kerrick (1981). A trapping pressure range of 0.50-0.53 GPa was estimated assuming a trapping temperature range of 500-520°C, suggested by quartz microstructures in the studied sample and temperature data of Célérier *et al.* (2009) and Spencer *et al.* (2012), from similar structural level within the MCTZ close to our sample localization. The obtained pressure values from the fluid inclusions in the present study are well comparable with the barometric data of c. 0.50-0.55 GPa reported in Spencer *et al.* (2012) for a strictly close sample. Our obtained pressure values are somewhat lower than those of Thakur *et al.* (2015; c. 0.60 GPa) even if it should be considered that their samples are located in a structurally higher position with respect to those reported in this paper. Moreover, our data are also in agreement with estimates of Sachan *et al.* (2001) which obtained temperature values of 530-560°C and pressure value of 0.60-0.65 GPa for the same structural setting, here investigated, along the Bhagirathi valley.

According to these findings it is likely that the here studied “early fluid” inclusions were trapped at the beginning of the MT activity, sampling circulating fluids near the pressure peak or the early stages of decompression. The water rich composition (0.12 X_{CO_2}) of these inclusions is also consistent with the stability of epidote within the veins host rocks, that requires water rich environment (e.g. Bucher & Grapes, 2011).

Finally, the entrapment pressure for the Munsiri Thrust “early fluid” inclusions supports that its activation was likely at shallower structural levels respect to the Vaikrita Thrust, where higher P-T conditions for shearing were reported (1.15 GPa and 580°C, Spencer *et al.*, 2012; 1.0 GPa and 650°C, Thakur *et al.*, 2015). This could suggest a progressively shift towards higher structural levels of accretion/deformation moving southward within the MCTZ.

ACKNOWLEDGEMENTS

This work was financially supported by the University of Pisa through the project P.R.A. 2016 (Resp. Montomoli C.).

REFERENCES

- AHMAD T., HARRIS N., BICKLE M., CHAPMAN H., BUNBORY J., PRINCE C., 2000. Isotopic constraints on the structural relationship between the Lesser Himalayan Series and the High Himalayan Crystalline Series, Garhwal Himalaya. *Geological Society of America Bulletin*, 112: 467-477.
- ANTOLIN B., APPEL E., MONTOMOLI C., DUNKL I., DIN L., GLOAGUEN R., EL BAY R., 2011. Kinematic evolution of the eastern Tethyan Himalaya: constraints from magnetic fabric and

- structural properties of the Triassic flysch in SE Tibet. In: Poblet J., Lisle R. (eds) Kinematic Evolution and Structural Styles of Fold-and-Thrust Belts. *Geological Society, London, Special Publications*, 349: 99-121.
- ARITA K., 1983. Origin of the inverted metamorphism of the lower Himalaya, central Nepal. *Tectonophysics*, 95: 43-60.
- BAKKER R.J., 2003. Package Fluids 1. Computer programs for analysis of fluid inclusion data and for modelling bulk fluid properties. *Chemical Geology*, 194: 3-23.
- BAKKER R.J., DIAMOND L.W., 2000. Determination of the composition and molar volume of H₂O-CO₂ fluid inclusions by microthermometry. *Geochimica et Cosmochimica Acta*, 64: 1753-1764.
- BORDET P., 1961. Recherches Géologiques dans l'Himalaya du Népal, Région du Makalu. *CNRS, Paris*.
- BUCHER K., GRAPES R., 2011. Petrogenesis of Metamorphic Rocks. *Eighth Edition. Springer, Berlin*.
- CAROSI R., GEMIGNANI L., GODIN L., IACCARINO S., LARSON K., MONTOMOLI C., RAI S.M., 2014. A geological journey through the deepest gorge on earth: The Kali Gandaki valley section, west-central Nepal. *Journal of the Virtual Explorer*, 47, paper 7.
- CAROSI R., MONTOMOLI C., IACCARINO S., MASSONNE H.-J., RUBATTO D., LANGONE A., GEMIGNANI L., VISONÀ D., 2016. Middle to late Eocene exhumation of the Greater Himalayan Sequence in the Central Himalayas: Progressive accretion from the Indian plate. *Geological Society of America Bulletin*, 128: 1571-1592, doi: 10.1130/B31471.1.
- CAROSI R., MONTOMOLI C., LANGONE A., TURINA A., CESARE B., IACCARINO S., FASCIOLI L., VISONÀ D., RONCHI A., RAI S., 2015. Eocene partial melting recorded in peritectic garnets from kyanite-gneiss, Greater Himalayan Sequence, central Nepal. In: Tectonics of the Himalaya. Eds. Mukherjee S., van der Beek P., Mukherjee P.K., *Geological Society London Special Publication*, 412: 111-119.
- CAROSI R., MONTOMOLI C., RUBATTO D., VISONÀ D., 2010. Late Oligocene high temperature shear zones in the core of the Higher Himalayan Crystallines (Lower Dolpo, western Nepal). *Tectonics*, 29: doi:10.1029/2008TC002400.
- CAROSI R., MONTOMOLI C., VISONÀ D., 2007. A structural transect in the Lower Dolpo: insights on the tectonic evolution of Western Nepal. *Journal of Asian Earth Sciences*, 29: 407-423.
- CATLOS E.J., HARRISON T.M., KOHN M.J., GROVE M., RYERSON F.J., MANNING C.E., UPRETI B.N., 2001. Geochronologic and thermobarometric constraints on the evolution of the Main Central Thrust, central Nepal Himalaya. *Journal of Geophysical Research*, 106: 16177-16204.
- CATLOS E.J., HARRISON T.M., MANNING C.E., GROVE M., RAI S.M., HUBBARD M.S., UPRETI B.N., 2002. Records of the evolution of the Himalayan orogen from in situ Th-Pb microprobe dating of monazite: Eastern Nepal and western Garhwal. *Journal of Asian Earth Sciences*, 20: 459-479.
- CÉLÉRIER J., HARRISON T.M., BEYSSAC O., HERMAN F., DUNLAP W.J., WEBB A.A.G., 2009. The Kumaun and Garhwal Lesser Himalaya, India; Part 2. Thermal and deformation histories. *Geological Society of America Bulletin*, 121: 1281-1297.
- COLCHEN M., LEFORT P., PÉCHER A., 1986. Carte Géologique Annapurna- Manaslu-Ganesh, Himalaya du Népal. *CNRS, Paris*, pp. 136.
- CORRIE S.L., KOHN M.J., 2011. Metamorphic history of the Central Himalaya, Annapurna region, Nepal, and implication for tectonic models. *Geological Society of America Bulletin*, 123: 1863-1879.
- DANIEL C.G., HOLLISTER L., PARRISH R.R., GRUJIC D., 2003. Exhumation of the Main Central thrust from lower crustal depths, Eastern Bhutan Himalaya. *Journal of Metamorphic Geology*, 21: 317-334.
- DARLING R.S., 1991. An extended equation to calculate NaCl contents from final clathrate melting temperatures in H₂O-CO₂-NaCl fluid inclusions: Implications for P-T isochore location. *Geochimica et Cosmochimica Acta*, 55: 3869-3871.
- DAVIDSON C., GRUJIC D., HOLLISTER L., SCHMID S.M., 1997. Metamorphic reaction related to decompression and syn-kinematic intrusion of leucogranite, High Himalayan Crystalline, Bhutan. *Journal of Metamorphic Geology*, 15: 593-612.
- DECELLES P.G., GEHRELS G.E., QUADE J., LAREAU B., SPURLIN M., 2000. Tectonic implications of U-Pb zircon ages of the Himalayan orogenic belt in Nepal. *Science*, 288: 497-499.
- DÈZES P., 1999. Tectonic and Metamorphic Evolution of the Central Himalayan Domain in Southeast Zaskar (Kashmir, India). *Ph.D. Thesis, Université de Lausanne*.
- DUNKL I., ANTOLÍN B., WEMMER K., RANTITSCH G., KIENAST, M., MONTOMOLI C., DING L., CAROSI R., APPEL E., EL BAY R., XU Q., VON EYNATTEN H., 2011. Metamorphic evolution of the Tethyan Himalayan flysch in SE Tibet. In: Growth and Collapse of the Tibetan Plateau. Eds. Gloaguen R., Ratschbacher L., *Geological Society of London Special Publications*, 353: 45-69.
- FERRILL D.A., MORRIS A.P., EVANS M.A., BURKHARDT M., GROSHONG R.H., ONASCH C.M., 2004. Calcite twin morphology: a low-temperature deformation geothermometer. *Journal of Structural Geology*, 26: 1521-1529.
- GAETANI M., GARZANTI E., 1991. Multicyclic history of the northern India continental margin (northwestern Himalaya). *American Association of Petroleum Geologists Bulletin*, 75: 1427-1446.
- GANSSER A., 1983. Geology of the Bhutan Himalaya. *Basel, Birkhäuser Verlag*, pp. 181.
- GODIN L., GRUJIC D., LAW R., SEARLE M.P., 2006. Crustal flow, extrusion, and exhumation in continental collision zones: an introduction. In: Channel Flow, Ductile Extrusion, and Exhumation in Continental Collision Zones. Eds. Law R., Searle M.P., Godin L., *Geological Society London Special Publications*, 268: 1-23.
- GROppo C., ROLFO F., LOMBARDO B., 2009. P-T evolution across the Main Central Thrust Zone (Eastern Nepal): hidden discontinuities revealed by petrology. *Journal of Petrology*, 50: 1149-1180.
- GURURAJAN N.S., CHOUDHURI B.K., 1999. Ductile Thrusting, metamorphism and Normal faulting in Dhauliganga Valley, Garhwal Himalaya. *Himalayan Geology*, 20: 19-29.
- HARRISON, T.M., RYERSON F.J., LE F.P., YIN, A., LOVERA, O.M., CATLOS, E.J., 1997. A late Miocene-Pliocene origin for the central Himalayan inverted metamorphism. *Earth and Planetary Science Letters*, 146: E1-E7.
- HEIM A.A., GANSSER A., 1939. Central Himalaya: Geological observations of the Swiss Expedition, 1936. *Delhi, India, Hindustan Publishing*, pp. 26.
- HODGES K.V., 2000. Tectonics of the Himalaya and southern Tibet from two perspectives. *Geological Society of America Bulletin*, 112: 324-350.

- HODGES K.V., SILVERBERG D.S., 1988. Thermal evolution of the Greater Himalaya, Garhwal, India. *Tectonics*, 7: 583-600.
- HUBBARD M.S., 1989. Thermobarometric constraints on the thermal history of the Main Central Thrust Zone and Tibetan Slab, eastern Nepal Himalaya. *Journal of Metamorphic Geology*, 7: 19-30.
- IACCARINO S., MONTOMOLI C., CAROSI R., MASSONNE H.-J., LANGONE A., VISONÀ D., 2015. Pressure-temperature-time-deformation path of kyanite-bearing migmatitic paragneiss in the Kali Gandaki valley (Central Nepal): Investigation of Late Eocene-Early Oligocene melting processes. *Lithos*, 231: 103-121.
- IACCARINO S., MONTOMOLI C., CAROSI R., MASSONNE H.-J., VISONÀ D., 2017. Geology and tectono-metamorphic evolution of the Himalayan metamorphic core: insights from the Mugu Karnali transect, Western Nepal (Central Himalaya). *Journal of Metamorphic Geology*, 35: 301-325, doi:10.1111/jmg.12233.
- JACOBS G.K., KERRICK D.M., 1981. A modified Redlich-Kwong equation for H₂O, CO₂, and H₂O-CO₂ mixtures at elevated pressures and temperatures. *American Journal of Science*, 281: 735-767.
- JAIN A.K., SHRESHTHA M., SETH P., KANYAL L., CAROSI R., MONTOMOLI C., IACCARINO S., MUKHERJEE P.K., 2014. The Higher Himalayan Crystallines, Alaknanda – Dhauliganga Valleys, Garhwal Himalaya, India. In: Geological field trips in the Himalaya, Karakoram and Tibet. Eds., Montomoli C., Carosi R., Law R., Singh S., Rai S.M., *Journal of the Virtual Explorer Electronic Edition*, 47.
- KOHN M.J., 2014. Himalayan Metamorphism and its Tectonic Implications. *Annual Review of Earth and Planetary Sciences*, 42: 381-419.
- KOHN M.J., CATLOS E.J., RYERSON F.J., HARRISON T.M., 2001. Pressure-temperature-time path discontinuity in the Main Central thrust zone, central Nepal. *Geology*, 29: 571-574.
- LARSON K.P., GODIN L., 2009. Kinematics of the Greater Himalayan sequence, Dhaulagiri Himal: implications for the structural framework of central Nepal. *Journal of the Geological Society*, 166: 25-43.
- LE FORT P., 1975. Himalaya: the collided range. *American Journal of Science*, 275: 1-44.
- MACFARLANE A.M., 1993. Chronology of tectonic events in crystalline core of the Himalaya, Langtang National Park, central Nepal. *Tectonics*, 12: 1004-1025.
- MARTIN A.J., 2016. A review of definitions of the Himalayan Main Central Thrust. *International Journal of Earth Science*, doi:10.1007/s00531-016-1419-8.
- MARTIN A.J., DECELLES P.G., GEHRELS G.E., PATCHETT P.J., ISACHSEN C., 2005. Isotopic and microstructural constraints on the location of the Main Central Thrust in the Annapurna range, central Nepal Himalaya. *Geological Society of America Bulletin*, 117: 926-944.
- MONTOMOLI C., CAROSI R., IACCARINO S., 2015. Tectonometamorphic discontinuities in the Greater Himalayan Sequence: a local or a regional feature? In: Tectonics of the Himalaya. Eds., Mukherjee S., van der Beek P., Mukherjee P.K., *Geological Society, London, Special Publication*, 412: 21-41.
- MONTOMOLI C., IACCARINO S., ANTOLIN B., APPLE E., CAROSI R., DUNKL I., DING L., VISONÀ D., 2017. Tectono-metamorphic evolution of the Tethyan Sedimentary Sequence (Himalayas, SE Tibet). *Italian Journal of Geosciences*, 136: 73-88, doi: 10.3301/IJG.2015.42.
- MONTOMOLI C., IACCARINO S., CAROSI R., LANGONE A., VISONÀ D., 2013. Tectonometamorphic discontinuities within the Greater Himalayan Sequence in Western Nepal (Central Himalaya): Insights on the exhumation of crystalline rocks. *Tectonophysics*, 608: 1349-1370.
- PARRISH R.R., HODGES K.V., 1996. Isotopic constraints on the age and provenance of the Lesser and Greater Himalayan sequences, Nepalese Himalaya. *Geological Society of America Bulletin*, 108: 904-911.
- PASSCHIER C.W., TROUW R.A.J., 2005. Microtectonics. *Second Edition*. Springer, Berlin.
- RICHARDS A., ARGLES T., HARRIS N., PARRISH R., AHMAD T., DARBYSHIRE F., DRAGANITS E., 2005. Himalayan architecture constrained by isotopic tracers from clastic sediments. *Earth and Planetary Science Letters*, 236: 773-796.
- ROBINSON D.M., 2008. Forward modeling the kinematic sequence of the central Himalayan thrust belt, western Nepal. *Geosphere*, 4: 785-801.
- ROBINSON D.M., DECELLES P.G., GARZIONE C.N., PEARSON O.N., HARRISON T.M., CATLOS E.J., 2001. The kinematic evolution of the Nepalese Himalaya interpreted from Nd isotopes. *Earth and Planetary Science Letters*, 192: 507-521.
- RUBATTO D., CHAKRABORTY S., DASGUPTA S., 2012. Timescales of crustal melting in the Higher Himalayan Crystallines (Sikkim, Eastern Himalaya) inferred from trace element-constrained monazite and zircon chronology. *Contributions to Mineralogy and Petrology*, doi: 10.1007/s00410-012-0812-y.
- SACHAN H.K., KOHN M.J., SAXENA A., CORRIE S.L., 2010. The Malari leucogranite, Garhwal Himalaya, northern India: chemistry, age, and tectonic implications. *Geological Society of America Bulletin*, 122: 1865-1876.
- SACHAN H.K., SAXENA A., VERMA P., RAI S.K., KHARYA A., 2013. Fluid Inclusion Study of the Higher Himalayan Quartzitic Pelites, Garhwal Himalaya, India: Implications for Recrystallization History of Metasediments. *Journal of Geological Society of India*, 82: 509-518.
- SACHAN H.K., SHARMA R., SAHAI A., GURURAJAN N.S., 2001. Fluid events and exhumation history of the main central thrust zone Garhwal Himalaya (India). *Journal of Asian Earth Sciences*, 19: 207-221.
- SAKLANI P.S., NAINWAL D.C., SINGH V.K., 1991. Geometry of the composite Main Central Thrust (MCT) in the Yamuna Valley, Garhwal Himalaya, India. *Neues Jahrbuch für Geologie und Palaeontologie: Monatshefte*, 1991: 364-380.
- SCHNEIDER C.A., RASBAND W.S., ELICEIRI K.W., 2012. NIH Image to ImageJ: 25 years of image analysis. *Nature methods*, 9: 671-675.
- SEARLE M.P., REX A.J., 1989. Thermal model for the Zaskar Himalaya. *Journal of Metamorphic Petrology*, 7: 127-134.
- SEARLE M.P., LAW R.D., GODIN L., LARSON K.P., STREULE M.J., COTTLE J.M., JESSUP M.J., 2008. Defining the Himalayan Main Central Thrust in Nepal. *Journal of the Geological Society, London*, 165: 523-534.
- SEARLE M.P., SIMPSON R.L., LAW R., PARRISH R.R., WATERS D.J., 2003. The structural geometry, metamorphic and magmatic evolution of the Everest massif, High Himalaya of Nepal-South Tibet. *Journal of the Geological Society, London*, 160: 345-366.
- SEARLE M.P., STEPHENSON B., WALKER J., WALKER C., 2007. Restoration of the Western Himalaya: implications for metamorphic

- protoliths, thrust and normal faulting, and channel flow models. *Episodes*, 30: 242-257.
- SEN K., CHAUDHURY R., PFÄNDER J., 2015. ^{40}Ar - ^{39}Ar age constraint on deformation and brittle-ductile transition of the Main Central Thrust and the South Tibetan Detachment zone from Dhauliganga valley, Garhwal Himalaya, India. *Journal of Geodynamics*, 88: 1-13.
- SPENCER C.J., HARRIS R.A., DORAIS M.J., 2012. The metamorphism and exhumation of the Himalayan metamorphic core, eastern Garhwal region, India. *Tectonics*, 31: 1-18.
- SPENCER C.J., HARRIS R.A., SACHAN H.K. SAXENA H., 2011. Depositional provenance of the Greater Himalayan Sequence, Garhwal Himalaya, India: Implications for tectonic setting. *Journal of Asian Earth Sciences*, 41: 344-354.
- STIPP M., STUNITZ H., HEILBRONNER R., SCHMID S.M., 2002. The eastern Tonale fault zone: A 'natural laboratory' for crystal plastic deformation over a temperature range from 250 to 700°C. *Journal of Structural Geology*, 24: 1861-1884.
- THAKUR S.S., PATEL S.C., SINGH A.K., 2015. A P-T pseudosection modelling approach to understand metamorphic evolution of the Main Central Thrust Zone in the Alaknanda valley, NW Himalaya. *Contribution to Mineralogy and Petrology*, 170: 1-26.
- TOURET J.L.R., 2001. Fluid inclusions in metamorphic rocks. *Lithos*, 55: 1-25.
- VALDIYA K.S., 1980. The two intracrustal boundary thrusts of the Himalaya. *Tectonophysics*, 66: 323-348.
- VANCE D., HARRIS N., 1999. Timing of prograde metamorphism in the Zaskar Himalaya. *Geology*, 27: 395-398.
- VANNAY J.C., GRASEMANN B., 1998. Inverted metamorphism in the High Himalaya of Himachal Pradesh (NW India): phase equilibria versus thermobarometry. *Schweizerische Mineralogische und Petrographische Mitteilungen*, 78: 107-132.
- VANNAY J.C., GRASEMANN B., RAHN M., FRANK W., CARTER A., BAUDRAZ V., COSCA M., 2004. Miocene to Holocene exhumation of metamorphic crustal wedges in the NW Himalaya: Evidence for tectonic extrusion coupled to fluvial erosion. *Tectonics*, 23: doi: 10.1029/2002TC001429.
- VISONÀ D., CAROSI R., MONTOMOLI C., PERUZZO M., TIEPOLO L., 2012. Miocene andalusite leucogranite in central-east Himalaya (Everest-Masang Kang area): low-pressure melting during heating. *Lithos*, 144: 194-208.
- WALKER J.D., MARTIN M.W., BOWRING S.A., SEARLE M.P., WATERS D.J., HODGES K.V., 1999. Metamorphism, melting, and extension: Age constraints from the High Himalayan Slab of southeast Zaskar and northwest Lahaul. *Journal of Geology*, 107: 473-495.
- YIN A., 2006. Cenozoic tectonic evolution of the Himalayan orogen as constrained by along-strike variation of structural geometry, exhumation history, and foreland sedimentation. *Earth-Science Reviews*, 76: 1-131.
- YIN A., HARRISON T.M., 2000. Geologic evolution of the Himalayan - Tibetan Orogen. *Annual Review of Earth and Planetary Science*, 28: 211-280.

(ms. pres. 28 agosto 2016; ult. bozze 25 ottobre 2016)

Edizioni ETS
Piazza Carrara, 16-19, I-56126 Pisa
info@edizioniets.com - www.edizioniets.com
Finito di stampare nel mese di marzo 2017